Carrier mobility model for organic semiconductors based on both Arrhenius and non-Arrhenius temperature dependence

L. G. WANG, Q. F. ZHANG, M. L. LIU*, Z. H. LIU, L. ZHANG
School of Electrical Engineering and Automation, Henan Key Laboratory of Intelligent Detection and Control of Coal Mine Equipment, Henan Polytechnic University, Jiaozuo, 454003, People's Republic of China

In this paper, we formulate a charge-carrier mobility model for disordered organic semiconductors based on both the Arrhenius and non-Arrhenius temperature dependence. This model can correctly reproduce the effects of temperature, electric field, and carrier concentration on the carrier mobility, and can rather well fit the numerical solution of the master equation at both the low carrier density and high carrier density, the latter of which cannot be well described using the extended Gaussian disorder model (EGDM). Furthermore, experimental current-voltage characteristics in devices based on organic semiconductors are also excellently reproduced by using this mobility model. These results further suggest that a temperature dependence of mobility given by the non-Arrhenius relation is suitable for the low carrier density and small energetic disorder limitation, and the high carrier density and large energetic disorder limitation gives the Arrhenius relation.

(Received July 8, 2025; accepted February 2, 2026)

Keywords: Charge transport, Mobility model, Temperature dependence, Disordered organic semiconductors

1. Introduction

Disordered organic semiconductors are promising materials for novel applications such as organic light emitting diodes, organic photovoltaics, and organic field effect transistors [1-8]. Physical insight of carrier transport in disordered organic semiconductors is vital for understanding the operating mechanisms of these devices [9-12]. The most important parameter characterizing the charge transport is the carrier mobility μ. A correct parametrization of the mobility is of vital importance for the development of algorithms desired to simulate devices based on disordered organic semiconductors. Theoretical equations for the mobility μ, dependent on temperature T, electric field E and carrier concentration p, are at the heart of the device simulation algorithms. The choice of the appropriate $\mu(T, p, E)$ suitable for applications in the device simulation software has been recently addressed in several studies [13-18]. In spite of the progress achieved in these studies, the parametrization of the dependences $\mu(T, p, E)$ still needs improvement.

So far, a well-established mobility model $\mu(T, p, E)$ was constructed by Pasveer et al., which is based on the non-Arrhenius temperature dependence $\ln(\mu) \propto 1/T^2$ and is known as the extended Gaussian disorder model (EGDM) [19]. Several review papers promote the EGDM as gold standard for the description of carrier mobility in disordered organic semiconductors, and the EGDM is the basis of commercially distributed device simulation software [14, 20, 21]. Although this mobility model is widely used, it is also heavily criticized [22-24]. The model deviates significantly from the simulated results based on the master equation, particularly in the regions of high carrier density and high electric field. Therefore, the state of research related to the theoretical description of the charge transport in disordered organic semiconductors can hardly be considered as satisfactory.

At present, a lack of consensus on the temperature dependence of the mobility in disordered organic semiconductors hampers progress toward the charge transport model. Theoretically, it has been demonstrated by Coehoorn et al. that within the Gaussian disorder model the charge transport is governed by the Arrhenius temperature dependence $\ln(\mu) \propto 1/T$ for high carrier density [25]. In contrast to Coehoorn et al., Bässler et al. showed a non-Arrhenius temperature dependence for the case of a Gaussian disorder model in the low density region [26]. Experimentally, mobility measured at the steady-state has shown Arrhenius temperature dependence [27, 28]. However, experiments under transient conditions such as the time-of-flight (TOF) measurement indicate that the non-Arrhenius temperature dependence can provide a more precise description of the mobility [29-31]. It has been known that the Arrhenius temperature dependence plays a more important role for the charge transport in the high density region. On the other hand, it has been argued that the charge transport is predominantly determined by the non-Arrhenius temperature dependence in the low

density region [32]. We believe that the above controversy, on the $\ln(\mu) \propto 1/T$ versus $\ln(\mu) \propto 1/T^2$ paradox, can be understood by using a unified description of mobility based on both the Arrhenius and non-Arrhenius temperature dependence.

In this paper, we will propose an improvement to the EGDM based on both the Arrhenius and non-Arrhenius temperature dependence, and to make a comparison between some results obtained from our model and the EGDM. It is shown that our approach can extend the results of the description of the mobility to the region of higher density and higher electric field. The rest of the paper is organized as follows. In Section 2, we explain some relevant theories and methods, and present an improved mobility model. In Section 3, we compare the theoretical results of current-voltage characteristics obtained from our model with experiments. Finally, a summary and conclusions are given in Section 4.

2. Models and methods

Within the extended Gaussian disorder model (EGDM) introduced by Pasveer et al. [19], the dependence of the mobility μ on temperature T, carrier concentration p, and electric field E can be written as

$$\mu(T, p, E) = \mu(T, p) f(T, E) \tag{1}$$

$$\mu(T, p) = \mu_{0,EGDM}(T) \exp\left[\frac{1}{2}(\hat{\sigma}^2 - \hat{\sigma})(2pa^3)^{\delta}\right] \tag{2}$$

$$\mu_{0,EGDM}(T) = 1.8 \times 10^{-9} \mu_0 \exp(-0.42\hat{\sigma}^2), \tag{3}$$

$$\delta \equiv 2[\ln(\hat{\sigma}^2 - \hat{\sigma}) - \ln(\ln 4)]/\hat{\sigma}^2, \quad \mu_0 \equiv a^2 \nu_0 e/\sigma, \tag{4}$$

$$f(T, E) = \exp\left\{0.44(\hat{\sigma}^{3/2} - 2.2)\left[\sqrt{1 + 0.8\left(\frac{eaE}{\sigma}\right)^2} - 1\right]\right\} \tag{5}$$

where $\mu(T, p)$ and $f(T, E)$ are density dependent and field dependent factor, $\mu_{0,EGDM}(T)$ is the temperature dependent mobility in the $E = 0$ and zero carrier density limit, $\hat{\sigma} = \sigma / k_B T$ is the dimensionless disorder parameter and σ is the width of the Gaussian density of states, a is the lattice constant, e is the charge of the carriers, ν_0 is the attempt-to-escape frequency.

It should be noted that the deviation of their model from the simulation numerical results is prominent, especially in the region of high carrier density and high electric field, as shown in the inset of Fig. 2 in Ref. [19]. It is clear that their model, only having a non-Arrhenius temperature dependence $\ln(\mu) \propto 1/T^2$ (see Eq. (3)), can well describe the charge transport at low density. The reason may be that the model neglects the influence of the Arrhenius temperature dependence $\ln(\mu) \propto 1/T$ on the charge transport at high carrier density. In fact, as mentioned in the Introduction, the non-Arrhenius temperature dependence governs the charge transport at low density and the Arrhenius temperature dependence becomes increasingly important at high density. Based on these results and our previous works [32], we propose an improved expression of the temperature dependent mobility based on both the Arrhenius and non-Arrhenius temperature dependence. The dependence of the mobility μ on carrier concentration p can be described as follows

$$\mu(T, p) = \mu_0(T) \exp\left(c_0 - \frac{1}{c_1 + c_2 (pa^3)^n}\right), \tag{6}$$

$$c_0 = -1.423\hat{\sigma}^2 + 14.38\hat{\sigma} - 29, \tag{7}$$

$$c_1 = \left(0.00285\hat{\sigma}^2 - 0.00824\hat{\sigma} + 0.106\right)/\left(\hat{\sigma} - 1.827\right), \tag{8}$$

$$c_2 = \left(0.016\hat{\sigma}^2 - 0.085\hat{\sigma} + 0.0\right)/\left(\hat{\sigma} - 1.69\right), \tag{9}$$

$$n = \left(5.403\hat{\sigma} - 3.914\right)/\left(\hat{\sigma}^2 + 18.4\hat{\sigma} - 29.4\right), \tag{10}$$

In Fig. 1, the mobility μ as a function of the carrier concentration p is plotted for various values of σ/k_BT at a vanishing electric field. The figure shows that Eqs. (6-10) can quite well fit the numerical results from the master equation, and give an improved description at high density as compared with the original model introduced by Pasveer et al. This indicates that there is a need to take the Arrhenius temperature dependence into account at high density.

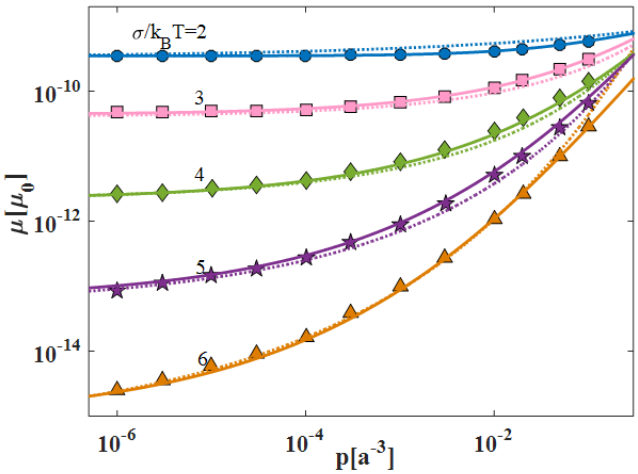

Fig. 1. Carrier concentration dependence of the mobility at various temperatures for a vanishing electric field. Symbols are numerical results from Ref. [19]. The dashed lines and solid lines represent theoretical fits using the parametrization scheme given in Eqs. (2) - (4) and Eqs. (6) - (10), respectively (colour online)

In the original model, Pasveer et al. adopt a density independent prefactor $f(T,E)$ to consider electric field dependence. However, it can be easily seen that for the most important temperature range $\hat{\sigma} > 1.69$, $f(T,E)$ gives incorrect limitation infinity as E tends infinity; whereas the correct limitation should be finite. In order to overcome the disadvantage, we introduce a weakly density dependent factor $g(T,E)$ in Eq. (11) to consider electric field dependence.

$$\mu(T,p,E) = \mu_0 \exp\left\{ g(T,E)\left[c_0 + d_0 - \frac{1}{c_1 + c_2 (pa^3)^n} \right] - d_0 \right\} \tag{11}$$

with $g(T, E)$ in the form:

$$g(T,E) = \left[1 + d_1 \left(\frac{Eea}{\sigma} \right)^2 \right]^{-1/2}, \tag{12}$$

where d_0 and d_1 are weakly density dependent parameters

$$d_0 = a_0 + a_1 * \ln(pa^3), \tag{13}$$

$$d_1 = 1.16 + 0.09 * \ln(pa^3), \tag{14}$$

Our fitting procedure shows that a_0 and a_1 can be well fitted by the following polynomials of reduced temperature:

$$a_0 = 0.076\hat{\sigma}^2 + 0.091\hat{\sigma} + 20.72, \tag{15}$$

$$a_1 = 0.035\hat{\sigma}^2 + 0.143\hat{\sigma} - 0.292, \tag{16}$$

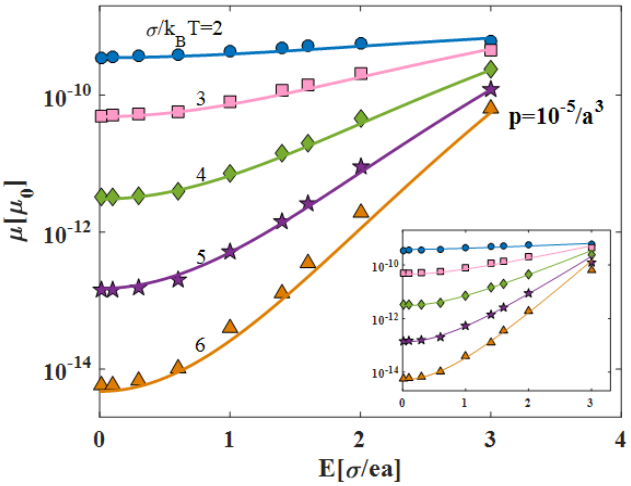

Fig. 2. Electric field dependence of the mobility at various temperatures for low densities in LEDs. Symbols are numerical results from Ref. [19]. The inset and main panel represent theoretical fits using the parametrization scheme given in Eqs. (1) - (5) and Eqs. (6)-(16), respectively (colour online)

In Fig. 2 and Fig. 3, we display the results for the mobility μ as a function of the electric field E at a low carrier density, $p = 10^{-5} / a^3$, typical for the operation regime of organic light-emitting diodes (LEDs), and a high carrier density, $p = 0.05 / a^3$, typical for the operation regime of organic field-effect transistors (FETs). From the figures we can see that the parametrization scheme is optimized for both the low density and high density region. Also it is shown that our parametrization scheme is significantly better than the results obtained by Pasveer et al. that only taking into account the non-Arrhenius temperature dependence [19], especially at high carrier density and high electric field. As compared to the EGDM, the improved model makes it possible to extend the results of the description of the mobility to the region of higher density and higher electric field. Therefore, it is demonstrated that our description of mobility by taking both the Arrhenius and non-Arrhenius temperature dependence into account is more applicable for disordered organic semiconductors.

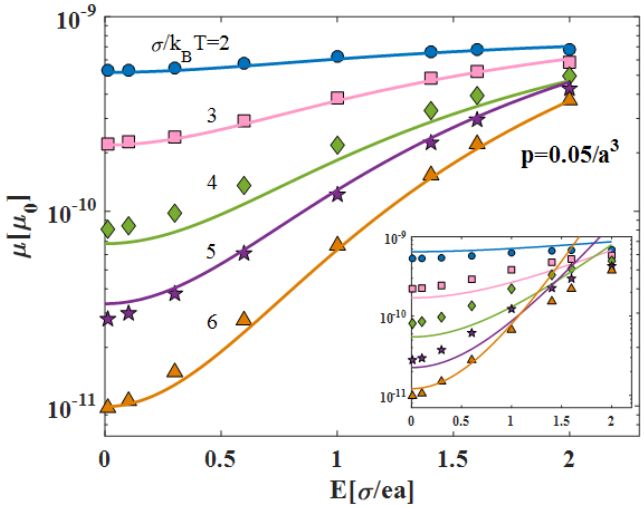

Fig. 3. Electric field dependence of the mobility at various temperatures for high densities in FETs. Symbols are numerical results from Ref. [19]. The inset and main panel represent theoretical fits using the parametrization scheme given in Eqs. (1) - (5) and Eqs. (6)-(16), respectively (colour online)

3. Results and discussion

Using the above parametrization scheme given in Eqs. (6-16), we now calculate the current-voltage ($J-V$) characteristics of MDMO-PPV hole-only device, PCBM electron-only device, MDMO-PPV:$PC_{61}BM$ hole-only and electron-only devices. The relation between the space charge limited current (SCLC) density J and voltage V can be obtained by numerically solving the following equations.

$$J = p(x) e \mu(T, p(x), E(x)) E(x), \tag{17}$$

$$\frac{dE}{dx} = \frac{e}{\varepsilon_0 \varepsilon_r} p(x), \tag{18}$$

$$V = \int_0^L E(x)dx, \tag{19}$$

where L is the active layer thickness sandwiched between two electrodes. X is the distance from the injecting electrode, ε_0 is the vacuum permeability, and ε_r is the relative dielectric constant of organic materials.

In Fig. 4, we display the solution of Eqs. (17)-(19) with the T, p, and E dependence on μ from the parametrization scheme given in Eqs. (6)-(16) and the experimental $J-V$ measurements of MDMO-PPV hole-only device. It can be seen that the temperature dependent $J-V$ characteristics can be well described using only one set of parameters: $\sigma = 0.13$ eV, $a = 1.5$ nm, and $\mu_0 = 1400$ m^2/Vs. The parameters σ, a and μ_0 are determined using a way that an optimal overall fit is obtained. The value of σ, (0.13 eV), is close to the result obtained by Pasveer et al. (0.14 eV) [19], and is consistent with the result obtained by van Mensfoort et al. [33]. The value of the lattice constant obtained in this work is smaller than the result obtained by Pasveer et al. (1.6 nm) [19], and is larger than the result from Martens et al. (1.2 nm) [34]. For the values of the parameters, Pasveer et al. pointed out that the lower value of σ can be mainly attributed to the omission of the p dependence and the lower value of a can be mainly attributed to the overestimation of the E dependence [19]. These results demonstrate that the more precise expression of mobility has an important impact on model parameters.

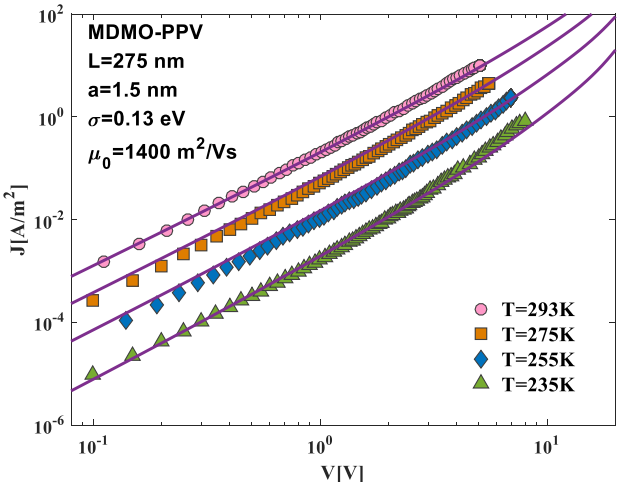

Fig. 4. Temperature dependent J-V characteristics of MDMO-PPV hole-only device. Symbols are experimental data from Ref. [19]. Lines are the numerical calculation results of the improved model (colour online)

Now we consider whether the improved model can also accurately describe the electron transport in disordered organic semiconductors. Fig. 5 shows the $J-V$ characteristics of a PCBM electron-only device as a function of temperature. The symbols and solid lines represent the experimental data and numerical calculations from the improved model, respectively. It is found that the temperature dependent $J-V$ characteristics of PCBM electron-only device can be well described using only one set of parameters: $\sigma = 0.064$ eV, $a = 4.5$ nm, and $\mu_0 = 1700$ m^2/Vs. This demonstrates that the improved model is applicable to the electron transport in disordered organic semiconductors.

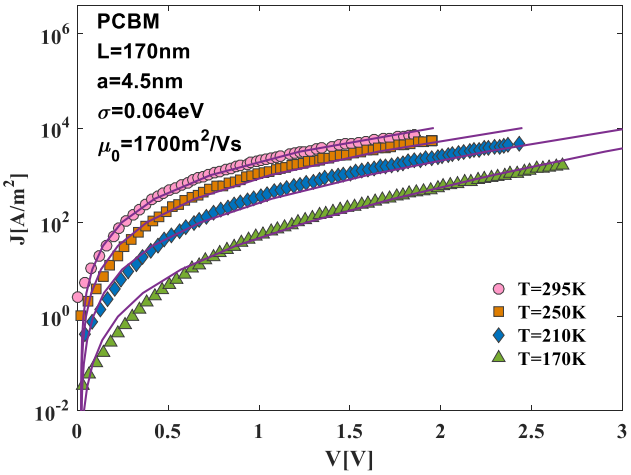

Fig. 5. Temperature dependent J-V characteristics of PCBM electron-only device. Symbols are experimental data from Ref. [35]. Lines are the numerical calculation results of the improved model (colour online)

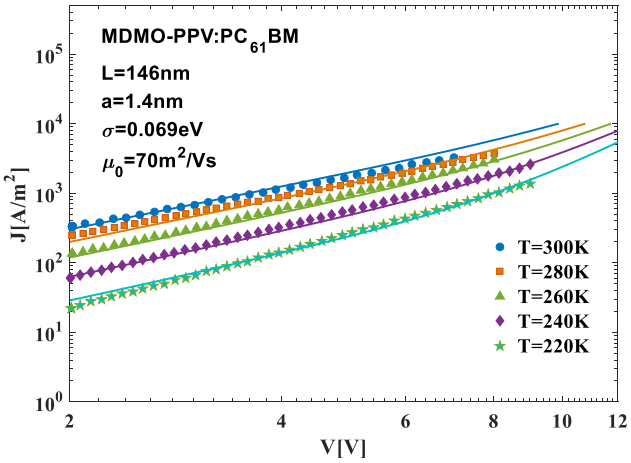

Fig. 6. Temperature dependent J-V characteristics of MDMO-PPV:$PC_{61}BM$ hole-only device. Symbols are experimental data from Ref. [36]. Lines are the numerical calculation results of the improved model (colour online)

Next, we will further investigate whether the improved model is also applicable to describe the charge transport in organic blends. Fig. 6 and Fig. 7 display the temperature dependent $J-V$ characteristics of hole-only and electron-only devices based on MDMO-PPV:$PC_{61}BM$ blend. From Fig. 6 and Fig. 7, it can be seen that the improved model fits the experimental data are very good for both hole-only and electron-only devices. The parameters of hole-only and electron-only devices are σ = 0.069 eV, a = 1.4 nm μ_0 = 70 m^2/Vs, and σ = 0.071 eV, a = 1.5 nm, μ_0 = 160 m^2/Vs, respectively. These results indicate that the improved model can also accurately describe the temperature dependent $J-V$ characteristics of both hole-only and electron-only devices based on MDMO-PPV:$PC_{61}BM$ blend. For MDMO-PPV, a hole mobility of 5×10^{-11} m^2/Vs at room temperature has been obtained [27]. For PCBM, an electron mobility of 2×10^{-7} m^2/Vs at room temperature has been obtained [35]. The electron mobility in PCBM is more than three orders of magnitude larger than the hole mobility in MDMO-PPV. It can be found from Fig. 6 and Fig. 7 that the current in MDMO-PPV:PCBM devices is significantly greater than that in MDMO-PPV device. Consequently, the dark current in MDMO-PPV:PCBM blend is completely dominated by electrons. Moreover, σ = 0.13 eV and σ = 0.064 eV for MDMO-PPV and PCBM, respectively, have been obtained in this work. The smaller σ of PCBM as compared to MDMO-PPV demonstrates that the energetic disorder is significantly smaller in PCBM, which gives rise to a higher mobility. These results indicate that lower energy disorder have higher mobility, demonstrating a close relationship between the mobility and energy disorder. Using Gaussian disorder in the improved model can reduce the influence of many processes into a single disorder parameter. It is shown that the degree of energy disorder appears to govern the charge transport in disordered organic semiconductors.

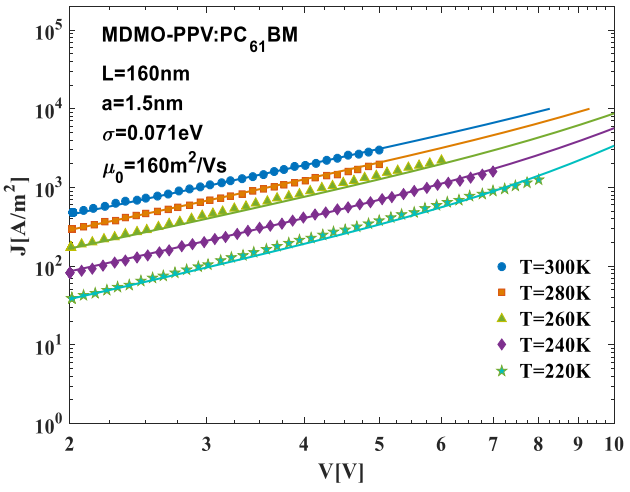

Fig. 7. Temperature dependent J-V characteristics of MDMO-PPV:$PC_{61}BM$ electron-only device. Symbols are experimental data from Ref. [36]. Lines are the numerical calculation results of the improved model (colour online)

4. Summary and conclusions

In summary, an improved unified description of the mobility dependent on temperature, electric field and carrier concentration is proposed based on both the Arrhenius and non-Arrhenius temperature dependence. The improved model provides a much better fit for the numerical results from the master equation than the original model introduced by Pasveer et al., especially at high carrier density and high electric field. This shows that our approach can extend the results of the description of the mobility to the region of higher densities and higher electric fields. Furthermore, we obtain the excellent fits with the experimental current-voltage characteristics of MDMO-PPV hole-only device, PCBM electron-only device, MDMO-PPV:$PC_{61}BM$ hole-only and electron-only devices by using the improved model. These results indicate that the improved model is suitable to study the charge transport in disordered organic semiconductors.

Acknowledgements

This work is supported by the Natural Science Foundation of Henan Province Grant No. 242300420282 and No. 242300420685, the Fundamental Research Funds for the Universities of Henan Province Grant No. NSFRF240818 and No. NSFRF240712, the Science and Technology Project of Henan Province Grant No. 252102211107.

References

[1] D. Scheunemann, C. Göhler, C. Tormann, K. Vandewal, M. Kemerink, Adv. Electron. Mater. **9**, 2300293 (2023).
[2] X. Ma, R. Ollearo, B. T. van Gorkom, C. H. L. Weijtens, M. Fattori, S. C. J. Meskers, A. J. J. M. van Breemen, R. A. J. Janssen, G. N. H. Gelinck, Adv. Funct. Mater. **33**, 2304863 (2023).
[3] B. V. Zee, Y. Li, G. J. A. H. Wetzelaer, P. W. M. Blom, Adv. Mater. **34**, 2108887 (2022).
[4] M. Li, D. K. Mangalore, J. Zhao, J. H. Carpenter, H. Yan, H. Ade, H. Yan, K. Müllen, P. W. M. Blom, W. Pisula, D. M. de Leeuw, K. Asadi, Nat. Commun. **9**, 451 (2018).
[5] F. H. Hasenburg, K. H. Lin, B. V. Zee, P. W. M. Blom, D. Andrienko, G. J. A. H. Wetzelaer, APL Materials **11**, 021105 (2023).
[6] N. B. Kotadiya, P. W. M. Blom, G. A. H. Wetzelaer, Phys. Rev. Appl. **11**, 024069 (2019).
[7] J. Wu, H. Cha, T. Du, Y. Dong, W. Xu, C. Lin, J. R. Durrant, Adv. Mater. **34**, 2101833 (2022).
[8] X. Ma, H. Bin, B. T. van Gorkom, T. P. A. van der Pol, M. J. Dyson, C. H. L. Weijtens,

M. Fattori, S. C. J. Meskers, A. J. J. M. van Breemen, D. Tordera, R. A. J. Janssen, G. H. Gelinck, Adv. Mater. **35**, 2209598 (2023).
[9] M. Van der Auweraer, F. C. De Schryver, P. M. Borsenberger, H. Bässler, Adv. Mater. **6**, 199 (1994).
[10] K. Vakhshouri, D. R. Kozub, C. Wang, A. Salleo, E. D. Gomez, Phys. Rev. Lett. **108**, 026601 (2012).
[11] N. Felekidis, A. Melianas, M. Kemerink, Org. Electron. **61**, 318 (2018).
[12] S. M. Hosseini, S. Wilken, B. Sun, F. Huang, S. Y. Jeong, H. Y. Woo, V. Coropceanu, S. Shoaee, Adv. Energy Mater. **13**, 2203576 (2023).
[13] T. Upreti, Y. Wang, H. Zhang, D. Scheunemann, F. Gao, M. Kemerink, Phys. Rev. Appl. **12**, 064039 (2019).
[14] Y. Lee, S. Jung, A. Plews, A. Nejim, O. Simonetti, L. Giraudet, S. D. Baranovskii, F. Gebhard, K. Meerholz, S. Jung, G. Horowitz, Y. Bonnassieux, Phys. Rev. Appl. **15**, 024021 (2021).
[15] J. X. Sun, H. C. Yang, Y. Li, H. J. Cui, Phys. Rev. Appl. **16**, 034037 (2021).
[16] J. O. Oelerich, D. Huemmer, S. D. Baranovskii, Phys. Rev. Lett. **108**, 226403 (2012).
[17] A. V. Nenashev, J. O. Oelerich, A. V. Dvurechenskii, F. Gebhard, S. D. Baranovskii, Phys. Rev. B **96**, 035204 (2017).
[18] J. O. Oelerich, A. V. Nenashev, A. V. Dvurechenskii, F. Gebhard, S. D. Baranovskii, Phys. Rev. B **96**, 195208 (2017).
[19] W. F. Pasveer, J. Cottaar, C. Tanase, R. Coehoorn, P. A. Bobbert, P. W. M. Blom, D. M. de Leeuw, M. A. J. Michels, Phys. Rev. Lett. **94**, 206601 (2005).
[20] R. Coehoorn, P. A. Bobbert, Phys. Status Solidi A **209**, 2354 (2012).
[21] M. Kuik, G. J. A. H. Wetzelaer, H. T. Nicolai, N. I. Craciun, D. M. De Leeuw, P. W. M. Blom, Adv. Mater. **26**, 512 (2014).
[22] A. V. Nenashev, F. Jansson, J. O. Oelerich, D. Huemmer, A. V. Dvurechenskii, F. Gebhard, S. D. Baranovskii, Phys. Rev. B **87**, 235204 (2013).
[23] S. D. Baranovskii, Phys. Status Solidi A **215**, 1700676 (2018).
[24] S. D. Baranovskii, A. V. Nenashev, D. Hertel, K. Meerholz, F. Gebhard, Phys. Rev. Appl. **22**, 014019 (2024).
[25] R. Coehoorn, W. F. Pasveer, P. A. Bobbert, M. A. J. Michels, Phys. Rev. B **72**, 155206 (2005).
[26] H. Bässler, Phys. Status Solidi B **175**, 15 (1993).
[27] P. W. M. Blom, M. C. J. M. Vissenberg, Mat. Sci. Eng. R **27**, 53 (2000).
[28] N. I. Craciun, J. Wildeman, P. W. M. Blom, Phys. Rev. Lett. **100**, 056601 (2008).
[29] D. Poplavskyy, J. Nelson, J. Appl. Phys. **93**, 341 (2003).
[30] H. Li, L. Chen, J. Qiao, L. Duan, D. Zhang, G. Dong, L. Wang, Y. Qiu, Sci. China Chem. **55**, 2428 (2012).
[31] C. Li, L. Duan, H. Li, Y. Qiu, J. Phys. Chem. C **118**, 10651 (2014).
[32] L. G. Wang, H. W. Zhang, X. L. Tang, C. H. Mu, The European Physical Journal B **74**, 1 (2010).
[33] S. L. M. van Mensfoort, S. I. E. Vulto, R. A. J. Janssen, R. Coehoorn, Phys. Rev. B **78**, 085208 (2008).
[34] H. C. Martens, P. W. M. Blom, H. F. M. Schoo, Phys. Rev. B **61**, 7489 (2000).
[35] V. D. Mihailetchi, J. K. J. van Duren, P. W. M. Blom, J. C. Hummelen, R. A. J. Janssen, J. M. Kroon, M. T. Rispens, W. J. H. Verhees, M. M. Wienk, Adv. Funct. Mater. **13**, 43 (2003).
[36] A. Melianas, N. Felekidis, Y. Puttisong, S. C. J. Meskers, O. Inganäs, W. M. Chen, M. Kemerink, Proceedings of the National Academy of Sciences of the United States of America **116**, 23416 (2019).

*Corresponding author: liuml1016@163.com